Online identification of pharmacodynamic parameters for closed-loop anesthesia with model predictive control

Bob Aubouin–Pairault, Mirko Fiacchini, Thao Dang

Online identification of pharmacodynamic parameters for closed-loop anesthesia with model predictive control

Bob Aubouin–Pairault[a,b,*], Mirko Fiacchini[a] and Thao Dang[b]

[a] Univ. Grenoble Alpes, CNRS, Grenoble INP, GIPSA-lab, Grenoble, 38000, France
[b] Univ. Grenoble Alpes, CNRS, Grenoble INP, VERIMAG, Grenoble, 38000, France

ARTICLE INFO

Keywords:
Closed-loop Anesthesia
Drug Control
Multi-Kalman Filters
Moving Horizon Estimator
Model Predictive Control
Uncertain Systems.

ABSTRACT

In this paper, a controller is proposed to automate the injection of propofol and remifentanil during general anesthesia using bispectral index (BIS) measurement. To handle the parameter uncertainties due to inter- and intra-patient variability, an extended estimator is used coupled with a Model Predictive Controller (MPC). Two methods are considered for the estimator: the first one is a multiple extended Kalman filter (MEKF), and the second is a moving horizon estimator (MHE). The state and parameter estimations are then used in the MPC to compute the next drug rates. The methods are compared with a PID from the literature. The robustness of the controller is evaluated using Monte-Carlo simulations on a wide population, introducing uncertainties in all parts of the model. Results both on the induction and maintenance phases of anesthesia show the potential interest in using this adaptive method to handle parameter uncertainties.

1. Introduction

The main objective of anesthesiologists during general anesthesia is to supervise and regulate the infusion rates of intravenous drugs to attain the required degree of hypnosis and analgesia while maintaining stable physiological parameters. With the emergence of fast-acting intravenous drugs like propofol and remifentanil, as well as the introduction of EEG-based hypnotic indicators such as the bispectral index (BIS), researchers have explored the possibility of automating the drug delivery process [1].

The goal of developing a closed-loop method for administering anesthesia drugs is to improve the patient's state evolution and reduce the workload for anesthesiologists. So far, studies have demonstrated the benefits of using closed-loop control for anesthesia drugs [2], [3], but research is ongoing to identify the best and most reliable control methods [4]. The task of automating drug dosage during general anesthesia is a complex and active area of research that has been a focus for the control community for over the last two decades. The high level of required reliability, along with the uncertain nature of the system, makes it a difficult task to design a controller. Numerous closed-loop control strategies have been proposed, see surveys [5] and [6] for instance. The main intravenous drug to induce and maintain hypnosis is propofol and most of the papers focus on the propofol-BIS single-input single-output (SISO) system, which is the kind of controller most widely clinically tested. However, the dosage paradigm employed during real surgery is much more complex, as the anesthesiologist needs to use remifentanil to induce analgesia, thus leading to the need to take into account the synergic effect between remifentanil and propofol [7] and the side effects of those drugs on the hemodynamic system. Although there is ongoing research on the subject, there does not exist yet a reliable indicator for the analgesia level. In this paper, the problem of designing a controller for the multiple-inputs, single-output (MISO) system propofol-remifentanil to BIS is addressed.

The problem of control design for propofol and remifentanil rates given the BIS measurements has already been studied during the last decade. In [8] and [9], an extended prediction self-adaptive control (EPSAC) has been designed using a linearized model of drug synergies, and simulations on a small set of patients have shown the superiority of this method compared to an approach with heuristic rules for the injection of remifentanil. In [10], a dual PID along with a heuristic-based approach has been clinically tested with good performance. Work [11] proposes a positive control law allowing real-time tuning of the propofol-remifentanil balance while ensuring stability. In [12], a Reinforcement Learning method has been used to address the challenge of the MISO system control design with simulation testing. The authors of [13] put forward a mid-range controller strategy that leverages the use of remifentanil for short-term and small-scale modulation of the bispectral index (BIS) while relying on propofol for longer-term interventions. This idea has been then formalized in [14] and [15] where an H_∞ and an MPC controller have been respectively tested with clinical trials and simulations. More recently in [16], [17], and [18], the authors have used the idea of fixing the ratio between drug flow rates to propose a PID and an MPC controller. To assess the robustness of those last controllers, uncertainties have been introduced in the model and Monte-Carlo simulations have been performed. The PID has been then clinically tested with promising results [19].

*Corresponding author
bob.aubouin-pairault@gipsa-lab.fr (B. Aubouin–Pairault); mirko.fiacchini@gipsa-lab.fr (M. Fiacchini); thao.dang@univ-grenoble-alpes.fr (T. Dang)
ORCID(s): 0000-0003-0029-438X (B. Aubouin–Pairault); 0000-0002-3601-0302 (M. Fiacchini); 0000-0002-3637-1415 (T. Dang)

In this study, either a multiple extended Kalman filter (MEKF) or a moving horizon estimator (MHE) is used to estimate both the state and the pharmacodynamic parameters of the patient model. The estimated parameters are then used in a model predictive controller (MPC) to compute the next drug rates. The use of MPC rather than simpler methods such as PID is motivated by the fact MPC can make use of the estimation of patient sensitivity to individualize the controller online and to obtain a controller easily adaptable to multiple-input multiple-output systems. In fact, uncertainties are the limiting factor for controller performance [20], and using a model updated online is a method to overcome this issue. Analogous ideas to deal with the model parametric uncertainties for reducing the inter-patient variability for the SISO system propofol-BIS have been considered in [21], [22] and more recently in [23]. The idea of using multiple Kalman filters to handle patient uncertainties has also been investigated in [24] to regulate mean arterial pressure and cardiac output in critical care subjects. The novelty of this approach, compared to the literature on this application, resides in a method that can address the uncertainties in the nonlinear functions involved in the anesthesia model. This research is intended as a preliminary investigation to demonstrate the feasibility of the control strategy before addressing more complex multiple-input multiple-output systems, where the mean arterial pressure could be used as an additional output, for instance.

The estimation methods used in this paper have been already presented and tested separately on clinical data in [25] and [26]. The first paper introduces the MHE method and tests it on clinical data. The second paper introduces MEKF and concludes that both MHE and MEKF have similar estimation performance indicators on simulated systems, while the MEKF outperforms the MHE on clinical data. In this paper, the estimation methods are appropriately adapted to improve the convergence of the BIS signal to the desired target. Moreover, the full closed-loop method is tested on both the induction and maintenance phases. Induction is the first part of the anesthesia when the patient falls asleep and corresponds to a set-point regulation problem. Maintenance corresponds to the surgical time when the state of the patient must remain as stable as possible; the control problem corresponds to a disturbance rejection task. Results are compared to the PID presented in [16]. A preliminary version of this work has been presented in [27] where only the MHE combined with MPC are compared to the PID on the induction phase.

The paper is organized as follows. In Section 2, the standard drug models for anesthesia are recalled, along with the associated uncertainties used in the simulations. Section 3 provides a comprehensive description of the estimation methods, while Section 4 describes the control design. Section 5 presents the simulation setup, the tuning of the different methods, and the associated results. Finally, Section 6 provides an analysis of those results, and Section 7 some concluding remarks.

2. Standard Anesthesia Model

Drug models involved in anesthesia dynamics modeling are usually composed of two parts: the pharmacokinetic (PK) and the pharmacodynamic (PD). The PK model describes the dynamics of the drug concentrations in the patient's body, whereas the PD one represents the link between the drug concentrations and their physiological effects.

2.1. Compartments Pharmacokinetic Model

For pharmacokinetic (PK) models of both drugs, propofol and remifentanil, a common approach is to use a four-compartment model. This model divides the body into three physical compartments: blood, muscles, and fat; and a virtual effect-site, as illustrated in Fig. 1. The compartment model results in a linear system represented by the following equations:

$$\begin{pmatrix}\dot{x}_1\\ \dot{x}_2\\ \dot{x}_3\\ \dot{x}_4\end{pmatrix} = \begin{pmatrix}-(k_{10}+k_{12}+k_{13}) & k_{12} & k_{13} & 0\\ k_{21} & -k_{21} & 0 & 0\\ k_{31} & 0 & -k_{31} & 0\\ k_e & 0 & 0 & -k_e\end{pmatrix}\begin{pmatrix}x_1\\ x_2\\ x_3\\ x_4\end{pmatrix} + \begin{pmatrix}\frac{1}{V_1}\\ 0\\ 0\\ 0\end{pmatrix} u \tag{1}$$

where x_1, x_2, x_3, and x_4 respectively represent the drug concentrations in blood, muscle, fat, and effect-site. The coefficients can be determined from Eq. (2) below, except for k_e which is not related to a physical meaning:

$$k_{10} = \frac{Cl_1}{V_1}, \quad k_{12} = \frac{Cl_2}{V_1}, \quad k_{13} = \frac{Cl_3}{V_1}, \quad k_{21} = \frac{Cl_2}{V_2}, \quad k_{31} = \frac{Cl_3}{V_3} \tag{2}$$

with V_i and Cl_i $(i = 1, 2, 3)$ respectively the volumes and the clearance rates of each compartment, which can be computed from a population-based model as in [28] and [29]. The input u is the drug infusion rate. In this paper, as in [16], the maximum infusion rate of propofol is $6.67 mg/s$ and that of remifentanil is $16.67 \mu g/s$. Next, the notation x_p and x_r for the states of the compartment models for propofol and remifentanil is used. Also, A_p, B_p, A_r, and B_r are the transition matrices of both drugs. Finally, both compartment models can be described by the decoupled system:

$$\begin{pmatrix}\dot{x}_p\\ \dot{x}_r\end{pmatrix} = \begin{pmatrix}A_p & 0_{4\times4}\\ 0_{4\times4} & A_r\end{pmatrix}\begin{pmatrix}x_p\\ x_r\end{pmatrix} + \begin{pmatrix}B_p & 0_{4\times1}\\ 0_{4\times1} & B_r\end{pmatrix}\begin{pmatrix}u_p\\ u_r\end{pmatrix}. \tag{3}$$

2.2. Pharmacodynamic Model

The impact of a drug concentration on the patient's hypnosis level is usually measured using the bispectral index (BIS). This indicator varies between 0 and 100, where 100 means a fully awake patient and 0 is a flat EEG. During surgery, the typical target range for BIS is between 40 and

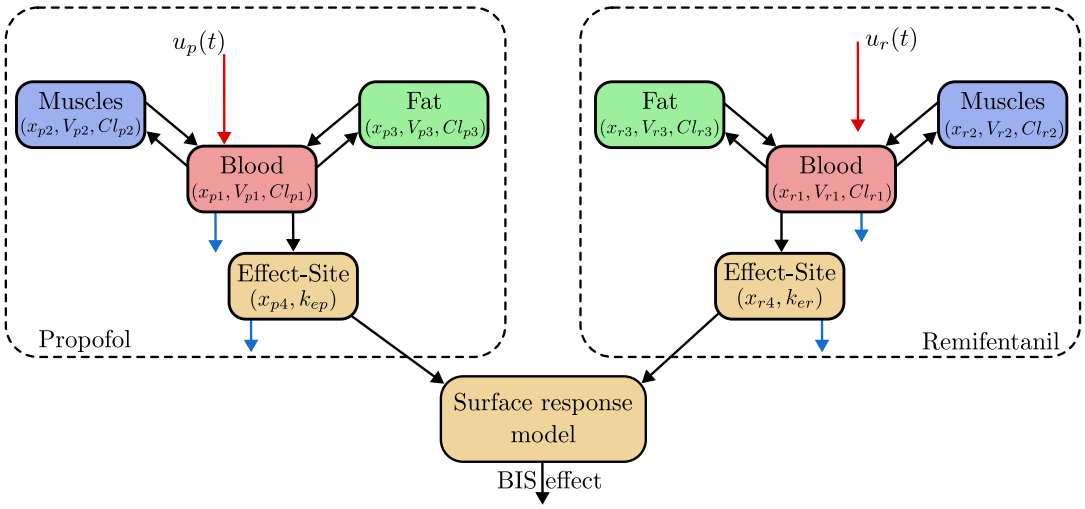

Figure 1: Scheme of the PK-PD compartments model

60 depending on the surgeon's need. From a modeling point of view, a Hill function is used to link drug concentration and drug effect on BIS. Due to the synergetic effect between propofol and remifentanil, the effect can be modeled as a response surface model [30]:

$$BIS(t) = E_0 \left(1 - \frac{I(t)^\gamma}{1 + I(t)^\gamma}\right) \tag{4}$$

with E_0 the initial BIS, γ the slope coefficient of the surface and $I(t)$ the interaction term defined by:

$$I(t) = \frac{x_{p4}(t)}{C_{50p}} + \frac{x_{r4}(t)}{C_{50r}}. \tag{5}$$

In these equations, x_{p4} and x_{r4} are the propofol and remifentanil concentrations of the effect-site, C_{50p} and C_{50r} are the propofol and remifentanil half-effect concentrations for BIS (*i.e.,* the concentrations to obtain half of the effect of the drugs).

Finally, the fully discretized model subject to noise can be summarized by the following structure:

$$\begin{cases} x(k+1) &= Ax(k) + Bu(k) \\ BIS(k) &= h(x(k)) + w(k) \end{cases} \tag{6}$$

where h is the non-linear output function from Eq. (4)-(5) and w models both the measurement noise and the output disturbances.

2.3. Model Parameters and Uncertainties

Several studies have been conducted in order to link the patient characteristics (age, height, weight, sex) to the PK parameters. The most recent are the models developed in [31] for propofol and in [32] for remifentanil. Those models have been validated on clinical datasets and include diverse populations. To simulate uncertainties in our testing procedure, Monte-Carlo simulations are used with a log-normal distribution for each parameter. The standard deviations used are those given in the papers cited above, nominal values are available in Table 1.

Table 1
Nominal values are for a woman of 75 kg, 165 cm, and 35 years old. Log std stands for logarithmic standard deviation.

	propofol		remifentanil	
	nominal	log std	nominal	log std
V_1	6.72	0.78	6.78	0.32
V_2	6.03	0.75	11.34	0.34
V_3	68.89	0.77	0.87	0.9
Cl_1	1.45	0.51	2.59	0.14
Cl_2	1.17	0.59	1.97	0.23
Cl_3	1.93	0.46	0.13	0.53
k_e	0.17	0.83	2.91	1.12

Table 2
Parameters of the log-normal distribution for the PD parameters

	nominal	log std
C_{50p}	4.47	0.18
C_{50r}	19.3	0.76
γ	1.43	0.30
E_0	97.4	0

For the response surface model, the values from [33] are used, as outlined in Table 2.

3. State and Parameter Estimation

As previously discussed, drug models are characterized by parameters that might significantly vary from patient to patient. It is then necessary to identify such parameters to improve the control performances, mostly when using controllers strongly relying on the model, as for model

predictive control employed here. To address this issue, two different estimators are proposed to estimate both the states and the unknown parameters of the output function. More particularly, a multiple extended Kalman filter (MEKF) and a moving horizon estimator (MHE) are proposed. Those two methods have been already presented and compared in [26] for this application. While the results were slightly better for MHE on simulated data, the MEKF method overperformed the MHE on clinical data.

Since the impact of PD variability uncertainty is more significant than PK variability uncertainty [34], the uncertain parameters of the PD system can be considered unknown and are represented by the vector $\theta = (C_{50p}, C_{50r}, \gamma)$. The estimation methods are used to estimate both the states and the parameters of the pharmacodynamic model, while the MPC is used to compute the control input to apply. The estimation methods have been improved with respect to [26] to ensure the convergence of the BIS signal to the desired target. In this section, the extended system considered in estimators is first described, then the two estimation methods are presented.

3.1. Extended System and Observability

Here, in addition to estimating the states of the system and the PD parameters, the estimator also estimates a disturbance added to the output to ensure the convergence of the closed loop. The considered states are $\bar{x} = \begin{pmatrix} x, & \theta, & d \end{pmatrix}$ and the model is given by:

$$\begin{aligned} \bar{x}(k+1) &= \bar{A}\bar{x}(k) + \bar{B}u(k) \\ BIS(k) &= h(x(k), \theta(k)) + d(k) = \bar{h}(\bar{x}(k)), \end{aligned} \tag{7}$$

with $\bar{A} = \begin{pmatrix} A & 0_{8\times4} \\ 0_{4\times8} & I_{4\times4} \end{pmatrix}$, $\bar{B} = \begin{pmatrix} B \\ 0_{4\times2} \end{pmatrix}$, and $\bar{h}$ the new output function parameterized by $\bar{x}$.

Analysing the observability of such a non-linear system is not trivial and non-linear tools must be used [35]. Computing the observability matrix, one can notice that this system is not directly observable. However, the two subsystems defined by the states $\begin{pmatrix} x, & \theta \end{pmatrix}$ and $\begin{pmatrix} x, & d \end{pmatrix}$ are structurally observable. This means that an optimal observer can either estimate $\begin{pmatrix} x, & \theta \end{pmatrix}$ or $\begin{pmatrix} x, & d \end{pmatrix}$ but not all the PD parameters and the disturbance at the same time. Thus, in the MHE, a time-dependent cost matrix will be used to either estimate either θ or d.

3.2. Multiple Extended Kalman Filter

To determine the pharmacodynamic (PD) parameters, the MEKF method employs a set of extended Kalman filter (EKF), with each filter corresponding to a specific realization of a vector selected from a grid in the parameter space. The grid is carefully designed to encompass the reasonable variability of the parameter vector. Following this, the active vector is chosen using a model-matching criterion. Fig. 2 illustrates the principle of the method.

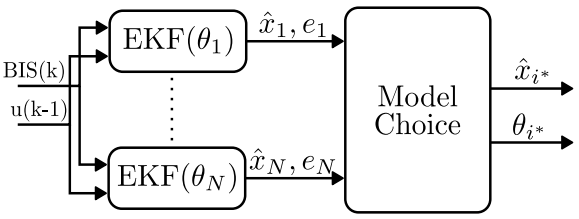

Figure 2: Multiple Extended Kalman Filter scheme

EKF is a state estimation method that relies on the linearization of a non-linear model [36]. The equations are the same as in a standard Kalman filter, except that the standard output matrix C, such that $y = Cx$, is not constant but time-dependent. The linearization is done around the previously estimated state $\hat{x}(k-1)$. In this paper the EKFs are parameterized by a scalar R_{MEKF} denoting the noise covariance and a matrix Q_{MEKF} denoting the model uncertainty covariance.

The aim of MEKF is to dynamically select the optimal observer at each time step, utilizing a criterion proposed in [37]. Originally designed for choosing an estimator among those with different gains, this method employs the estimation error on the output, denoted as $e_i(k) = BIS(k) - h(\hat{x}(k), \theta_i)$ for the filter i, to construct a selection criterion for each observer. The dynamics of the criterion for the i^{th} observer are expressed as follows:

$$\eta_i(k+1) = \nu\eta_i(k) + |e_i(k)|^2 + \lambda|K_i(k)e_i(k)|^2. \tag{8}$$

Here, λ, and $\nu \in [0, 1]$ are positive design parameters, and $K_i(k)$ is the gain of each EKF at the time step k. The criterion is dependent on both the output estimation error $e_i(k)$ and the correction effort of the observer $K_i(k)e_i(k)$. The following equation can be deduced from Eq. (8):

$$\eta_i(k) = \nu^k\eta_i(0) + \sum_{j=0}^{k-1} \nu^{k-j-1}(|e_i(j)|^2 + \lambda|K_i(j)e_i(j)|^2). \tag{9}$$

where η_i can be interpreted as a cost and the objective is to choose the observer with the minimal cost at each time step, denoted by i^*.

To prevent frequent switches between observers, a parameter $\epsilon \in (0, 1]$ is introduced. A switch occurs at time step k only if there exists $i \neq i^*$ such that $\eta_i(k) < \epsilon\eta_{i^*}(k)$.

3.3. Moving Horizon Estimator

The MHE is an optimal observer that estimates the states and the parameters of the system by minimizing a cost function [38]. This cost function uses a fixed number N_{MHE} of past measurements and control inputs. The advantage of this method is that it can directly deal with non-linear systems and constraints on the states. Due to the non-linearity of the system, the convergence of the optimization is not guaranteed. However, the estimator can estimate the states and the parameters of the system with good accuracy, as

shown in [25]. The cost function of the MHE at time step k is given by:

$$J_N(\bar{\mathbf{x}}, \hat{\bar{x}}(k-N_{MHE}), \mathbf{BIS}, \mathbf{u}) = \sum_{i=k-N_{MHE}}^{k} \|BIS(i) - \bar{h}(\bar{x}(i))\|^2_{R_{MHE}} + \sum_{i=k-N_{MHE}+1}^{k} \|\bar{x}(i) - (\bar{A}\bar{x}(i-1) + \bar{B}u(i-1))\|^2_{Q} + \|\bar{x}(k-N_{MHE}) - \hat{\bar{x}}(k-N_{MHE})\|^2_{P(k)}$$

where $\bar{\mathbf{x}}$ represents the state over the estimation horizon (decision variable) up to time k and $\hat{\bar{x}}(k-N_{MHE})$ is the previously estimated state at time $k-N_{MHE}$. Note that in this equation and in the following of the paper, bold notation is used to represent sequences of variables. The remaining arguments, namely **BIS** and **u**, represent the output and the input measurements profiles over the estimation horizon, Q_{MHE}, R_{MHE}, and P represent the penalty matrices, and N_{MHE} is the length of the estimation window. Note that, as [25], the time-varying penalty matrix P has been tuned for modulating in time the priorities of either the PD parameters or the disturbance estimations, to overcome observability issues. P is a diagonal matrix where the non-constant term is given by:

$$p^{MHE}_{jj}(k) = \beta^j_1 + \beta^j_2 e^{-\beta^j_3 e^{-\beta^j_4 k}}, \tag{10}$$

for $j \in \{9, 10, 11, 12\}$. β^j_i are real, tuned to prioritize either the estimation of the PD parameter θ or the disturbance d. The final MHE optimization problem is given by:

$$\begin{aligned} \hat{\bar{\mathbf{x}}}(k) = \arg\min_{\bar{\mathbf{x}}} \quad & J_{MHE}(\bar{\mathbf{x}}) \\ \text{subject to} \quad & \bar{x}(k+i+1) = \bar{A}\bar{x}(k+i) + \bar{B}u(k+i) \\ & \text{for } i \in [-N_{MHE}, -1]. \end{aligned} \tag{11}$$

Note that both estimators are initialized with a null concentration and the nominal PD parameters at the beginning of the anesthesia. Thus, the first injection is only dependant on the control part of the close loop, which is presented in the next section.

4. Controller Design

The novelty of this paper is to use the estimators coupled to a Model Predictive Control (MPC) strategy, the overall control scheme is given in Fig 3.

Since the problem is a set-point tracking problem, the equilibrium that the MPC should target must be computed first, as illustrated in the next section. Afterward, the MPC is presented and, finally, the PID controller used as a baseline is described.

4.1. Equilibrium Computation

The equilibrium control input u_{eq} is designed to stabilize the system at a desired BIS level. Due to the long-time

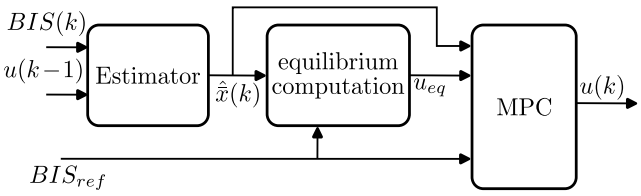

Figure 3: Control scheme

constants of the slow compartments in the pharmacokinetic (PK) model, such as muscle and fat, the control input is computed to stabilize only the blood and effect site compartments of each drug. The drug concentrations in the slow compartments are assumed to remain constant within the near future. This separation between fast and slow compartments is justified by the fact that the slow compartments take hours to converge, whereas the concentrations to be controlled stabilize in a few minutes. With this purpose, the following matrices are defined for each drug:

$$A_{fast} = \begin{pmatrix} -(k_{10}+k_{12}+k_{13}) & 0 \\ k_e & -k_e \end{pmatrix}, \quad B_{fast} = \begin{pmatrix} 1/V_1 \\ 0 \end{pmatrix}, \quad E_{slow} = \begin{pmatrix} k_{12} & k_{13} \\ 0 & 0 \end{pmatrix}, \tag{12}$$

where k_{10}, k_{12}, k_{13}, and k_e are the coefficients of the PK model and V_1 is the volume of the blood compartment. The equilibrium input for one drug at time t should respect this equation:

$$A_{fast}\begin{pmatrix} x_{1,eq} \\ x_{4,eq} \end{pmatrix} + B_{fast}u_{eq} + E_{slow}\begin{pmatrix} x_2(t) \\ x_3(t) \end{pmatrix} = 0. \tag{13}$$

Consider now the matrices for both drugs:

$$A_{eq} = \begin{pmatrix} A_{fast,p} & 0_{2\times2} \\ 0_{2\times2} & A_{fast,r} \end{pmatrix}, B_{eq} = \begin{pmatrix} B_{fast,p} & 0_{2\times2} \\ 0_{2\times2} & B_{fast,r} \end{pmatrix}, E_{eq} = \begin{pmatrix} E_{slow,p} & 0_{2\times2} \\ 0_{2\times2} & E_{slow,r} \end{pmatrix}. \tag{14}$$

The fast and slow state vectors are denoted $x_{fast} = (x_{p1}, x_{p4}, x_{r1}, x_{r4})$ and $x_{slow} = (x_{p2}, x_{p3}, x_{r2}, x_{r3})$, respectively. Note that the output of the system (6) only depends on the fast states.

The equilibrium control input u_{eq} is computed at each step to consider the current estimated values of both the PD parameter and the slow state vector. The following optimization problem (denoted as equilibrium computation

in Fig. 3) is thus solved online:

$$
\begin{aligned}
(u_{eq}, x_{fast,eq}) = \arg\min_{u, x_{fast}} & \left(BIS_{ref} - \tilde{h}\big(x_{fast}, \hat{\theta}(k), \hat{d}(k)\big) \right)^2 \\
& + \left(u_p \sqrt{r_1^{MPC}} - u_r \sqrt{r_2^{MPC}} \right)^2 \\
\text{subject to} \quad & A_{eq} x_{fast} + B_{eq} u + E_{eq} \hat{x}_{slow}(k) = 0 \\
& u \in \mathbb{U},
\end{aligned}
$$

where u_p, and u_r are the elements of the vector u, and $\mathbb{U}$ is the set of feasible control inputs, as specified in Section 2. Thus, u_{eq} is the control input that stabilizes the system at BIS_{ref} according to the estimated PD parameters. $\tilde{h}$ is the output function parameterized by x_{fast}, θ, and d. Moreover, $\hat{\theta}(k)$, $\hat{d}(k)$, and $\hat{x}_{slow}(k)$ are the observed PD parameters, disturbance, and slow states at time step k. In this equation r_1^{MPC} and r_2^{MPC} are chosen to set the ratio between u_p and u_r at the equilibrium. They are similar to the role of r in the PID, in fact, $r = \sqrt{r_2^{MPC}/r_1^{MPC}}$.

4.2. Model Predictive Control

Model Predictive Control is an advanced control method that consists of solving online an optimization problem to obtain the optimal control input in the presence of constraints on the state and the input [39]. In the case of set-point tracking, MPC often employs the precomputed value of the target equilibrium state and input, see Section 4.1.

In our case, though, using $x_{fast,eq}$ as concentration targets in the MPC could degrade the control performance. In fact, due to the uncorrelated dynamics of propofol and remifentanil, this approach would decouple the MPC into two independent tracking problems. Although this method is computationally simpler, as it removes all nonlinearities, it is less efficient since achieving the BIS target is the real control objective rather than attaining the equilibrium concentrations. For instance, if propofol is overdosed, leading to a concentration excess, an uncorrelated MPC would not reduce the remifentanil dose to compensate for it, as the controller aims only at the equilibrium concentrations. This limitation is significant given the asymmetry in the available control inputs, where negative rates are not allowed. Therefore, the difference between the predicted BIS and the target BIS is directly employed in the MPC problem cost. While there are no convergence guarantees for this nonlinear optimization problem, it leads to good performances in practice, as demonstrated later.

Thus, the cost of the optimization problem is given by:

$$
\begin{aligned}
J_{MPC}(\bar{\mathbf{x}}, \mathbf{u}) = \sum_{i=1}^{N_{MPC}} & \| BIS_{ref} - \bar{h}(\bar{x}(k+i)) \|^2 \\
& + \| u(k+i) - u_{eq} \|^2_{R_{MPC}},
\end{aligned}
\tag{15}
$$

where $\bar{\mathbf{x}}$, and $\mathbf{u}$ are respectively the predicted states and control inputs over the prediction horizon. BIS_{ref} is the BIS target (50 in our simulation), $R_{MPC} = diag(r_1^{MPC}, r_2^{MPC})$ is the input weighting matrix, N_{MPC} is the prediction horizon and u_{eq} is the equilibrium control input computed as in Section 4.1.

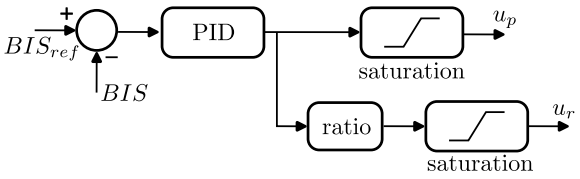

Figure 4: PID controller

The final optimization problem of the MPC is given by:

$$
\begin{aligned}
\mathbf{u} = \arg\min_{\mathbf{u}} \quad & J_{MPC}(\bar{\mathbf{x}}, \mathbf{u}) \\
\text{subject to} \quad & \bar{x}(k+i+1) = \bar{A}\bar{x}(k+i) + \bar{B}u(k+i) \\
& \quad \text{for } i \in [0, N_{MPC} - 1] \\
& u(k+i) \in \mathbb{U} \quad \text{for } i \in [0, N_{MPC} - 1] \\
& \bar{x}(k) = \hat{\bar{x}}(k).
\end{aligned}
\tag{16}
$$

Then at each step time, the control input $u(k)$ applied to the patient is the first element of the optimal control input $\mathbf{u}$.

With the proposed formulation of MPC, the inputs converge to proportional drug rates at the equilibrium, but during the transition, the balance between propofol and remifentanil is managed implicitly by the optimization problem. Thus, the concentration of propofol and remifentanil might be different than that produced by a controller with a controller using a strict proportional relation between both drug rates.

4.3. PID Controller

The PID controller, presented in [16] and illustrated in Fig. 4, is used as a benchmark to compare the performances of the proposed control scheme. In this method, the rates of propofol and remifentanil are proportional, and the fixed ratio between the two drugs is given by r ($u_r = r \cdot u_p$). The control input is computed as follows:

$$
u_p(t) = K_p \left(e(t) + \frac{1}{T_i} \int_0^t e(\tau) d\tau + T_d \frac{de(t)}{dt} \right), \tag{17}
$$

where $e(t)$ is the regulation error defined by $e(t) = BIS_{ref} - BIS(t)$. Before applying the control input to the patient, the outputs of the controller are saturated to satisfy the constraint of the system. Additionally, an anti-windup strategy is used to prevent integration wind-up. Two different sets of parameters are used, one for each phase of anesthesia (induction and maintenance). During the parameter switch from induction to maintenance, the PID states are reset to ensure continuous control.

5. Closed-loop Simulations

In this section, three controllers are tested, using the same tuning method and scenario to ensure a fair comparison.

5.1. Simulation Setup and Performance Criteria

To evaluate the performances of the controllers, simulations are conducted with 1000 different patients using random uniform sampling to determine age, gender, height, and weight. Age is between 18 and 70 years old, height between 150 and 190cm, and weight between 50 and 100kg. Uncertainties are then introduced to both the PK and PD models through log-normal sampling, as described in Section 2.3. The simulation consists of an induction phase followed by a maintenance phase starting at a time equal to 10 minutes, incorporating a step disturbance of +10 in BIS at 10 minutes and -10 at 15 minutes, resulting in a total simulation time of 20 minutes. This simple disturbance, previously utilized in the literature, allows one to evaluate the disturbance rejection performance of the controller. To simulate the system in conditions similar to the real clinical ones, a sampling time of one second is used for the patient simulation and estimation, and the control period is set to five seconds, as in the real implementation of the PID made recently in [40]. Additionally, white noise with a standard deviation of 3, filtered by a second-order low-pass filter with a cutoff frequency of 0.03 Hz, is added to the output.

The performance criteria differ from those typically used in the literature, as criteria more relevant to clinical practice are selected. For the induction phase, the criteria include:

- **IAE:** Integral of the absolute error between BIS and the reference.
- **Sleep Time:** Time to achieve and maintain a BIS level lower than 60.
- **Low BIS time:** Time spent with BIS value lower than 40.
- **Lower BIS value:** Minimum BIS value reached.
- **Settling time:** Time to reach and maintain the interval [40;60].
- **Drug doses:** Total volume of propofol and remifentanil used relative to the patient's weight.

For the maintenance phase, the criteria include:

- **IAE:** Integral of the absolute error between BIS and the reference.
- **Time out of range:** Time spent with BIS outside the interval [40;60].
- **Lower BIS value:** Minimum BIS value reached.
- **Higher BIS value:** Maximum BIS value reached.
- **Drug doses:** Total volume of propofol and remifentanil used relative to the patient's weight.

The optimization problems are solved using CASADI software [41] with IPOPT solver. The entire simulation code presented in this paper is written in Python and is available at `https://github.com/BobAubouin/TIVA_Drug_Control`, utilizing [42] for execution.

5.2. Controller Tuning

For tuning, $N_{patient} = 32$ random patients are considered, not included in the set of 1000 used for testing. Demographic data for patients in the train and the test set are illustrated in Fig. 5. One can observe that the training distribution reflects the distribution of the test set. Each controller is tuned using the same criterion, given by:

$$J = \underset{i=1,\dots,N_{patient}}{\text{mean}} \left(\sum_{k=1}^{N_{sim}} f_{cost}(BIS_i(k), BIS_{ref}, k) \right) \quad (18)$$

with:

$$f_{cost}(x, y, k) = \begin{cases} (x-y)^2 & \text{if } x > y - 10 \text{ or } k \cdot t_s \geq 600 \\ |x-y|^{2.6} & \text{otherwise} \end{cases}$$

where BIS_{ref} is the reference BIS value (50), $BIS_i(t)$ is the BIS value of patient i at time step k, and t_s is the sampling time. This specific asymmetric cost function is chosen to penalize undershooting during the induction phase, to prevent overly aggressive controllers, and to obtain a time to sleep between two and three minutes. Sustained BIS values below 40 are particularly undesirable, as they are associated with post-operative morbidities [43]. The cost is symmetric during maintenance since, in this phase, it is equally important to avoid excessively deep or light hypnosis.

All controllers are tuned using a tree-structured Parzen estimator from [44], a black-box optimization method selected for its ability to handle both continuous and discrete parameters, especially in large hyperparameter spaces.

For PID tuning, the propofol-to-remifentanil rate ratio is set to two, a common value. Subsequently, all parameters are tuned for both induction and maintenance, resulting in six hyperparameters. For MEKF-MPC and MHE-MPC, the estimator and controller are jointly tuned. For MPC, the three hyperparameters are the prediction horizon (N_{MPC}) and the control weighting matrix (R_{MPC}) for induction and maintenance. Note that the ratio between the diagonal coefficients of R_{MPC} is fixed to achieve behavior similar to that of PID, specifically $\sqrt{r_2^{MPC}/r_1^{MPC}} = 2$. For MEKF, the tuning parameters include λ, ϵ, R_{MEKF} (the scalar representing output noise covariance for the EKF), and q_{MEKF} (a scalar multiplying the matrice Q_{MEKF} of state uncertainties covariance in the EKF). For MHE, the tuning parameters are the prediction horizon (N_{MHE}) and the weighting scalar R_{MHE}.

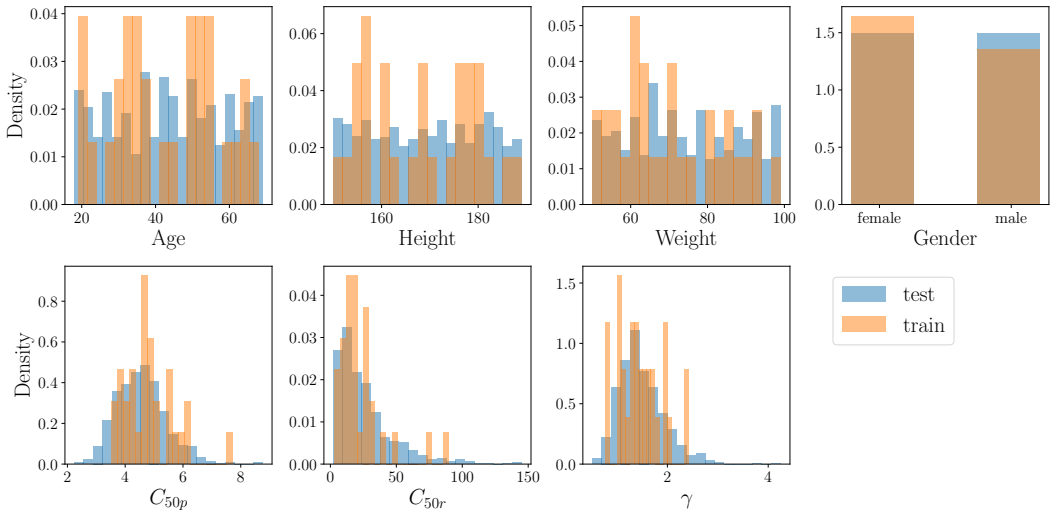

Figure 5: Demographic patient density for both the train and the test set.

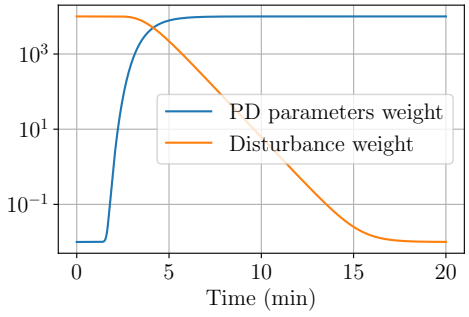

Figure 6: Time-varying weights in P matrix used in the MHE to penalize PD parameters and disturbance estimation.

For MHE, note that the parameters of Eq. (10) have been tuned to first identify the PD parameters during induction and then to estimate the disturbance. The resulting time-dependant weights are illustrated on Fig. 6.

5.3. Results

The mean and standard deviation of the simulation trajectories for 1000 patients are depicted in Fig. 7 for the three controllers. Moreover, specific results for the three controllers are presented in Table 3.

Regarding the computational resources, the methods are quite disparate with a mean step time duration of *0.01ms* for PID, *63ms* for MEKF-MHE, and *43ms* for MHE-MPC. Despite the use of three optimization problems for the MHE-MPC method against two in the MEKF-MPC method, the MHE is faster using the optimized parameters.

Performance criteria of the three controllers for the specific phase of induction are available in Table. 4, and in Table 5 for the maintenance phase.

Table 3
General results for the tested controllers. The cost is computed over 1000 patients.

Controller	Proposed cost ($\times 10^{-4}$) mean ± std	max	Percentage of patients with BIS under 40
PID	15.4 ± 10.0	89.7	11.1%
MEKF-MPC	14.0 ± 9.4	80.8	12.3%
MHE-MPC	11.2 ± 8.0	104.2	10.4%

The concentrations of propofol and remifentanil in the effect site concentration are available in Fig. 8.

Finally, Fig. 9, 10, and 11 show the dependency of the total IAE, the sum of induction and maintenance IAE, with respect to patient age, gender, and patient drug sensitivity. Note that the impact of gender on the performance of MHE-MPC is significant ($t(998) = -2.09$, $p < 0.05$, using a student test to confirm the hypothesis).

6. Discussion

For induction, results indicate that the MPC methods outperform the PID in terms of IAE, with a 24% reduction in mean IAE between MHE-MPC and PID. While this is already a significant improvement the difference in terms of IAE is less pronounced than the one in terms of the proposed cost in Eq. (18) as shown in Table 3 where the cost is reduced by 27% over the whole simulation. This difference demonstrates the importance of the tuning cost which should be carefully chosen according to the specification. The MHE-MPC achieves to reach both the fastest mean sleep time and the minimum mean time under a BIS of 40, denoting a better trade-off between these two opposite performance criteria. The MEKF-MPC method is a bit better than the PID in terms of IAE but is far from the MHE-MPC

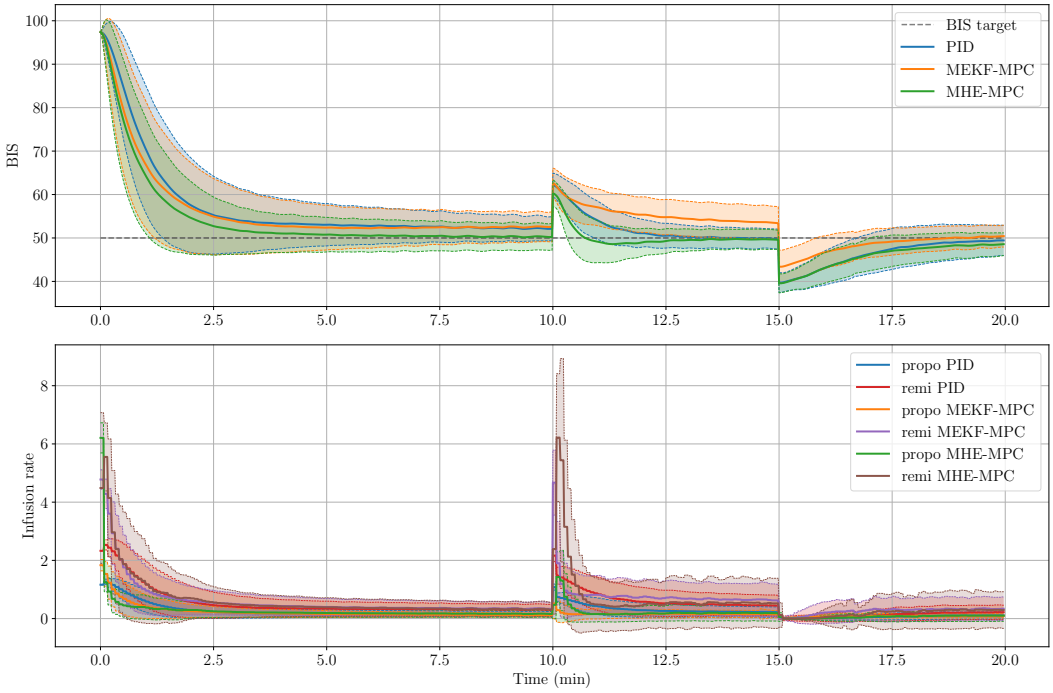

Figure 7: Mean BIS across 1000 patients for the three controllers. The plot displays the mean value ± standard deviation.

Table 4
Performance criteria for the three controllers in the induction phase.

Controller	**IAE** mean ± std	max	**Sleep Time** (m) mean ± std	**Settling time** (m) mean ± std	**Low BIS time** (s) mean ± std	max	**Lower BIS** mean ± std	min	**Propo volume** (mg/kg) mean ± std	max	**Remi volume** ($\mu g/kg$) mean ± std	max
PID	5151 ± 2140	14842	2.4 ± 2.0	2.7 ± 2.2	10.4 ± 43.0	468.0	46.3 ± 5.4	19.7	2.3 ± 1.0	10.0	4.6 ± 2.1	19.9
MEKF-MPC	4847 ± 2255	16946	2.6 ± 2.6	2.9 ± 2.6	9.7 ± 37.3	353.0	46.1 ± 5.9	18.3	2.0 ± 1.0	9.4	5.2 ± 2.2	20.9
MHE-MPC	3900 ± 1723	12055	1.7 ± 1.6	2.0 ± 2.0	8.0 ± 35.9	386.0	44.6 ± 4.5	13.0	2.4 ± 1.0	8.3	5.4 ± 2.9	26.7

performances. However, the MHE-MPC method reaches an average lower BIS value. Its good performance also comes at the cost of increased consumption of remifentanil, although the propofol consumption is similar, leading to higher effect-site concentration as shown in Fig. 8. While this is an important point to consider, it could be addressed in the future by introducing constraints on drug concentration in the MPC optimization problem.

Looking at the extreme values, one can observe that MHE-MPC gets the worst undershoot and also obtains the worst proposed cost. However, the controller with a longer time with a BIS below 40 is the PID with more than seven minutes below the threshold.

For maintenance, the MHE-MPC method also outperforms the other methods with 10% improvement of IAE and 30% less time out of range compared to PID. The MEKF-MPC obtains the worst mean IAE due to a long convergence time after the positive disturbance as visible in Fig. 7. Despite those differences, all the controllers obtain correct performances which fulfill the clinical requirements.

Concerning the impact of age on the controller's performance, Fig. 9 shows that the mean total IAE increases with age. This is particularly true for the MEKF-MPC method which becomes worse than PID for the group older than fifty years old. The PID method manages to obtain a similar

Table 5
Performance criteria for the three controllers in the maintenance phase.

Controller	**IAE** mean ± std	max	**Time out of range** (s) mean ± std	max	**Lower BIS** mean ± std	min	**Higher BIS** mean ± std	max	**Propo volume** (mg/kg) mean ± std	max	**Remi volume** ($\mu g/kg$) mean ± std	max
PID	2532 ± 995	5634	64.7 ± 68.4	348.0	38.0 ± 2.2	30.4	63.1 ± 2.5	74.7	1.6 ± 0.8	7.8	3.3 ± 1.6	15.6
MEKF-MPC	2664 ± 1053	10266	55.2 ± 72.5	596.0	41.5 ± 3.1	32.8	63.6 ± 3.4	80.6	1.0 ± 0.6	5.7	4.4 ± 2.1	17.2
MHE-MPC	2268 ± 660	5227	44.2 ± 40.9	294.0	37.6 ± 2.2	25.0	61.2 ± 2.7	72.6	1.2 ± 0.6	4.7	4.1 ± 2.1	19.5

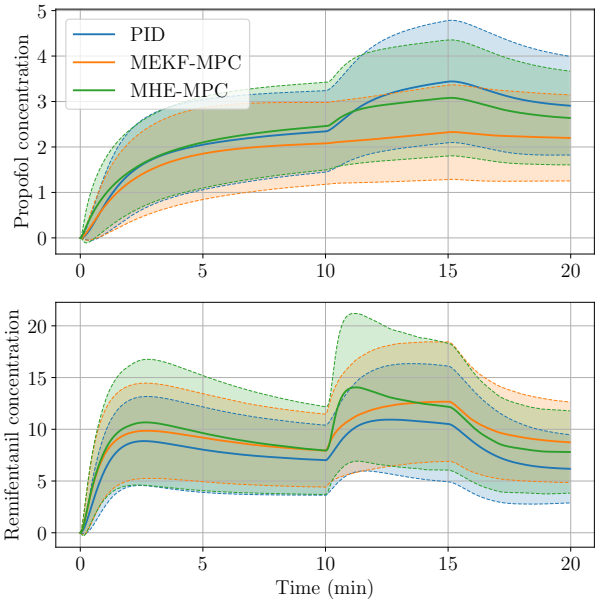

Figure 8: Mean propofol (in $\mu g/mL$) and remifentanil (ng/mL) in concentrations across 1000 patients. The plot displays the mean value ± standard deviation.

performance for all the groups younger than sixty years old. Nevertheless, the worst performance of the MHE-MPC still outperforms the best performance of PID. This graph denotes the disparity of performance across different groups of patients. On the same topic, on Fig. 10 one can observe that all methods perform better on female than on male.

Fig. 11 shows how the dependence of the total IAE on the patient sensitivity, expressed by the half effect concentration of each drug. Although C_{50p} does not seem to be a major determinant factor of the total IAE, C_{50r} is well correlated with the performance criterion (an analogous test on the slope coefficient γ reveals no correlation either). One can notice looking at this figure that the MHE-MPC methods manage to reduce this dependency on these parameters thanks to the online identification process.

Both the conclusions about age and patient sensitivity on controller performance must be taken carefully due to the high level of variability in those results and the important number of variables to consider. A proper statistical analysis could be performed in the future to obtain more insightful assessments.

Overall, the MHE-MPC outperforms the other tested methods. However, its increased remifentanil consumption during induction and computational complexity compared to PID warrants careful consideration for clinical implementation. Despite the MEKF-MPC's inferior performances, previous studies [26] have demonstrated its superiority over MHE on clinical data, suggesting its potential suitability for clinical trials.

The study is also affected by some limitations:

- The simulated population is not representative of a real population due to the uncorrelated and uniform sampling of the demographic data. If this is a way to partially reproduce the real world complexity in our dataset, it is also a problem since those results will not fully represent clinical trial populations.
- The simulation might not represent accurately the real world. First, if noise has been identified from clinical data it could be different in practice. Moreover, this study does not consider a delay from BIS measurement while it might be considered such as in [45]. Finally, the probabilistic distribution used to sample patient parameters might not be representative. For the pharmacodynamic part, values have been extracted from [33], a study including only twenty patients. In this sense, the variability of C_{50r} might be exaggerated.
- The three controllers compared in this study might not be directly applicable in practice. Some aspects such as missing measurements or low signal quality index are not considered here. Moreover, an effort to reduce the number of drug rate changes could be done with event-based control such as in [46] to obtain a behaviour closer to the anesthesiologist actions.
- In the study, a population-based PID has been used as a baseline but an individualized version has also been proposed by the same authors in [17]. The simple version has been used since easier to implement. The individualized version might better handle different patients as recently demonstrated in [47].
- Finally, comparing PID and MPC methods using only performance criteria might not be fair and one should also consider the importance of the PID sobriety which allows a fast understanding, implementation, and maintenance of this method compared to MPC-based methods.

Conclusion

In this paper, a novel control method for the co-administration of propofol and remifentanil driven by BIS measurement has been proposed. The method consists of an extended estimator along with a model predictive controller to regulate the patient's depth of hypnosis. Two estimation methods are compared: the Multiple Extended Kalman Filter and the Moving Horizon Estimator, alongside a PID controller used as a baseline. Results obtained from simulations involving 1000 virtual patients are discussed using the proposed performance criteria.

These findings underscore the efficacy of the MHE-MPC method during the induction and maintenance phase, where it strikes a better balance between convergence speed and

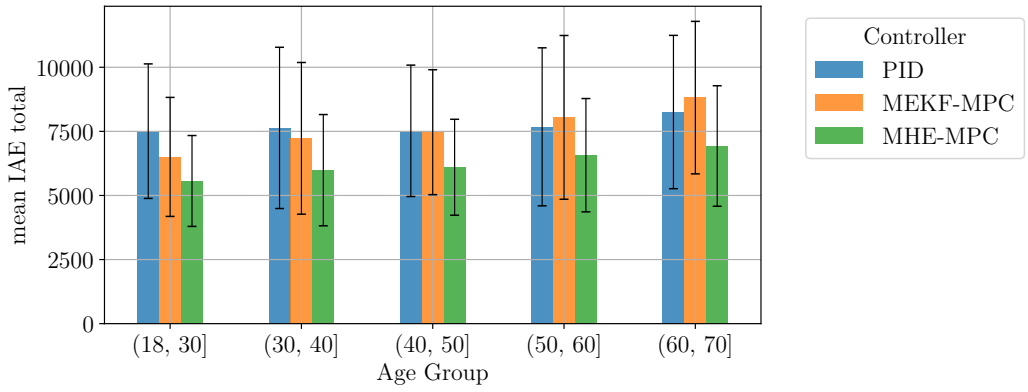

Figure 9: Mean total IAE for different age groups for the three controllers. Error bars denote the standard deviation.

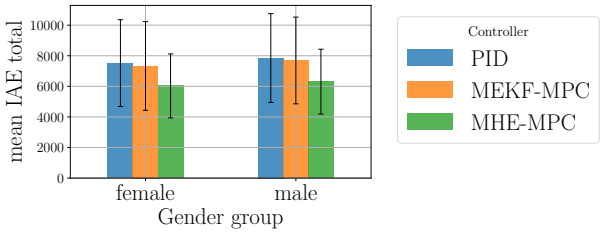

Figure 10: Mean total IAE for the two genders for the three controllers. Error bars denote the standard deviation.

overshoot compared to MEKF-MPC and PID control. However, the bigger consumption of remifentanil coupled with the complexity of the method temper the overall efficacy of the MPC approach.

Beyond evaluating specific control methods, this paper demonstrates the feasibility of conducting fair comparisons among closed-loop methods using clinically relevant indicators. Furthermore, it highlights the importance of the controller tuning and thus the choice of the cost function for tuning. While it is not intended to replace clinical trials, comparison using numerical simulation allows the controllers to be tested under standardized conditions. This is a first step to ensure the reliability of the control method before moving to clinical trials. We believe that the open-source philosophy should be encouraged in the research community as it is a key point to ensure the reproducibility of the results, further comparisons and trust within the clinical community.

Declaration of Competing Interest

The authors declare no conflict of interest.

Declaration of Generative AI and AI-assisted technologies in the writing process

During the preparation of this work the authors used ChatGPT in order to improve readability and language. After using this tool, the authors reviewed and edited the content as needed and take full responsibility for the content of the publication.

Acknowledgment

This work has been partially supported by the LabEx PERSYVAL-Lab (ANR-11-LABX-0025-01) funded by the French program Investissement d'avenir. All (or most of) the computations presented in this paper were performed using the GRICAD infrastructure (link), which is supported by Grenoble research communities.

CRediT authorship contribution statement

Bob Aubouin–Pairault: Conceptualization of this study, Investigation, Software, Visualization, Writing - original draft. **Mirko Fiacchini:** Conceptualization of this study, Methodology, Supervision, Project administration, Funding acquisition, Writing - review and editing. **Thao Dang:** Supervision, Funding acquisition, Writing - review and editing.

References

[1] D. Copot, *Automated Drug Delivery in Anesthesia*. Academic Press, 2020.

[2] E. Brogi, S. Cyr, R. Kazan, F. Giunta, and T. M. Hemmerling, "Clinical Performance and Safety of Closed-Loop Systems: A Systematic Review and Meta-analysis of Randomized Controlled Trials," *Anesthesia & Analgesia*, vol. 124, pp. 446–455, Feb. 2017.

[3] L. Pasin, P. Nardelli, M. Pintaudi, M. Greco, M. Zambon, L. Cabrini, and A. Zangrillo, "Closed-Loop Delivery Systems Versus Manually Controlled Administration of Total IV Anesthesia: A Meta-analysis of Randomized Clinical Trials," *Anesthesia & Analgesia*, vol. 124, pp. 456–464, Feb. 2017.

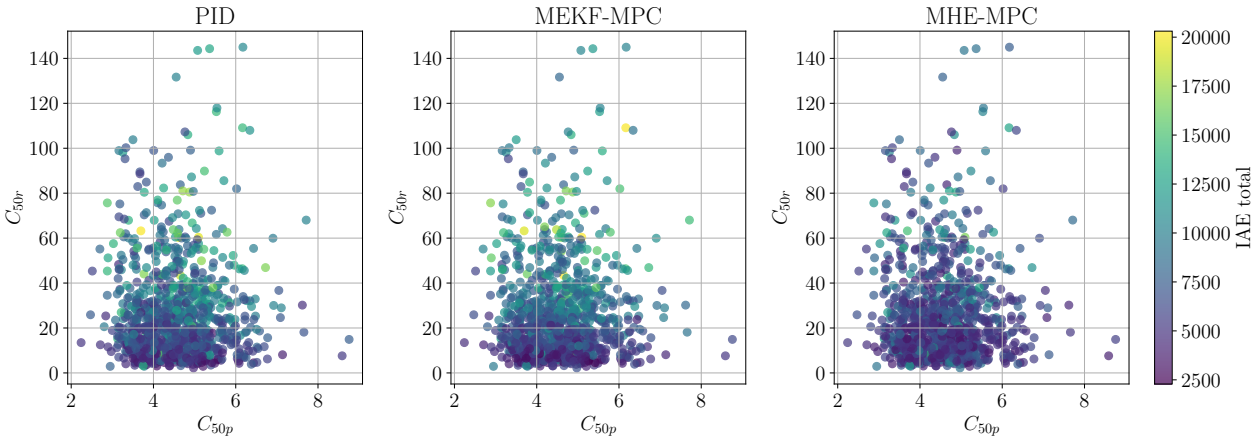

Figure 11: Total IAE for each controller, regarding patient PD parameters (C_{50p} and C_{50r}).

[4] R. G. Loeb and M. Cannesson, "Closed-Loop Anesthesia: Ready for Prime Time?," *Anesthesia & Analgesia*, vol. 124, pp. 381–382, Feb. 2017.

[5] M. Singh and G. Nath, "Artificial intelligence and anesthesia: A narrative review," *Saudi Journal of Anaesthesia*, vol. 16, no. 1, pp. 86–93, 2022.

[6] M. Ghita, M. Neckebroek, C. Muresan, and D. Copot, "Closed-Loop Control of Anesthesia: Survey on Actual Trends, Challenges and Perspectives," *IEEE Access*, vol. 8, pp. 206264–206279, 2020.

[7] D. Copot, R. D. Keyser, and C. Ionescu, "Drug Interaction Between Propofol and Remifentanil in Individualised Drug Delivery Systems," *IFAC-PapersOnLine*, vol. 48, pp. 64–69, Jan. 2015.

[8] C. Ionescu, J. Tenreiro Machado, R. De Keyser, J. Decruyenaere, and M. M. R. F. Struys, "Nonlinear dynamics of the patient's response to drug effect during general anesthesia," *Communications in Nonlinear Science and Numerical Simulation*, vol. 20, pp. 914–926, Mar. 2015.

[9] I. Nascu, C. M. Ionescu, I. Nascu, and R. De Keyser, "Evaluation of three protocols for automatic DOA regulation using Propofol and Remifentanil," in *2011 9th IEEE International Conference on Control and Automation (ICCA)*, pp. 573–578, Dec. 2011.

[10] N. Liu, T. Chazot, S. Hamada, A. Landais, N. Boichut, C. Dussaussoy, B. Trillat, L. Beydon, E. Samain, D. I. Sessler, and M. Fischler, "Closed-Loop Coadministration of Propofol and Remifentanil Guided by Bispectral Index: A Randomized Multicenter Study," *Anesthesia & Analgesia*, vol. 112, pp. 546–557, Mar. 2011.

[11] F. N. Nogueira, T. Mendonça, and P. Rocha, "Controlling the depth of anesthesia by a novel positive control strategy," *Computer Methods and Programs in Biomedicine*, vol. 114, pp. e87–e97, May 2014.

[12] R. Padmanabhan, N. Meskin, and W. M. Haddad, "Reinforcement learning-based control for combined infusion of sedatives and analgesics," in *2017 4th International Conference on Control, Decision and Information Technologies (CoDIT)*, pp. 0505–0509, Apr. 2017.

[13] N. West, K. van Heusden, M. Görges, S. Brodie, A. Rollinson, C. L. Petersen, G. A. Dumont, J. M. Ansermino, and R. N. Merchant, "Design and Evaluation of a Closed-Loop Anesthesia System With Robust Control and Safety System," *Anesthesia & Analgesia*, vol. 127, pp. 883–894, Oct. 2018.

[14] K. van Heusden, J. M. Ansermino, and G. A. Dumont, "Robust MISO Control of Propofol-Remifentanil Anesthesia Guided by the NeuroSENSE Monitor," *IEEE Transactions on Control Systems Technology*, vol. 26, pp. 1758–1770, Sept. 2018.

[15] N. Eskandari, K. van Heusden, and G. A. Dumont, "Extended habituating model predictive control of propofol and remifentanil anesthesia," *Biomedical Signal Processing and Control*, vol. 55, p. 101656, Jan. 2020.

[16] L. Merigo, F. Padula, N. Latronico, M. Paltenghi, and A. Visioli, "Optimized PID control of propofol and remifentanil coadministration for general anesthesia," *Communications in Nonlinear Science and Numerical Simulation*, vol. 72, pp. 194–212, June 2019.

[17] M. Schiavo, F. Padula, N. Latronico, M. Paltenghi, and A. Visioli, "Individualized PID tuning for maintenance of general anesthesia with propofol and remifentanil coadministration," *Journal of Process Control*, vol. 109, pp. 74–82, Jan. 2022.

[18] A. Pawłowski, M. Schiavo, N. Latronico, M. Paltenghi, and A. Visioli, "Model predictive control using MISO approach for drug co-administration in anesthesia,"

Journal of Process Control, vol. 117, pp. 98–111, Sept. 2022.

[19] M. Schiavo, F. Padula, N. Latronico, M. Paltenghi, and A. Visioli, "A modified PID-based control scheme for depth-of-hypnosis control: Design and experimental results," *Computer Methods and Programs in Biomedicine*, vol. 219, p. 106763, June 2022.

[20] J. M. Gonzalez-Cava, F. B. Carlson, O. Troeng, A. Cervin, K. van Heusden, G. A. Dumont, and K. Soltesz, "Robust PID control of propofol anaesthesia: Uncertainty limits performance, not PID structure," *Computer Methods and Programs in Biomedicine*, vol. 198, p. 105783, Jan. 2021.

[21] R. D. Keyser, D. Copot, and C. Ionescu, "Estimation of Patient Sensitivity to Drug Effect during Propofol Hypnosis," in *2015 IEEE International Conference on Systems, Man, and Cybernetics*, pp. 2487–2491, Oct. 2015.

[22] F. Padula, C. Ionescu, N. Latronico, M. Paltenghi, A. Visioli, and G. Vivacqua, "Inversion-based propofol dosing for intravenous induction of hypnosis," *Communications in Nonlinear Science and Numerical Simulation*, vol. 39, pp. 481–494, Oct. 2016.

[23] Y. Wahlquist, K. van Heusden, G. A. Dumont, and K. Soltesz, "Individualized closed-loop anesthesia through patient model partitioning," in *2020 42nd Annual International Conference of the IEEE Engineering in Medicine Biology Society (EMBC)*, pp. 361–364, July 2020.

[24] R. Rao, B. Aufderheide, and B. Bequette, "Experimental studies on multiple-model predictive control for automated regulation of hemodynamic variables," *IEEE Transactions on Biomedical Engineering*, vol. 50, pp. 277–288, Mar. 2003.

[25] K. Moussa, B. Aubouin-Pairault, M. Alamir, and T. Dang, "Data-Based Extended Moving Horizon Estimation for MISO Anesthesia Dynamics," *IEEE Control Systems Letters*, vol. 7, pp. 3054–3059, 2023.

[26] B. Aubouin-Pairault, M. Fiacchini, and T. Dang, "Comparison of multiple Kalman filter and moving horizon estimator for the anesthesia process," *Journal of Process Control*, vol. 136, p. 103179, Apr. 2024.

[27] B. Aubouin–Pairault, M. Fiacchini, and T. Dang, "PID and Model Predictive Control Approach for Drug Dosage in Anesthesia During Induction: A Comparative Study," in *PID24 - 4th IFAC Conference on Advances in Proportional-Integral-Derivative Control*, (Almeria, Spain), IFAC - International Federation of Automatic Control, June 2024.

[28] T. W. Schnider, C. F. Minto, S. L. Shafer, P. L. Gambus, C. Andresen, D. B. Goodale, and E. J. Youngs, "The Influence of Age on Propofol Pharmacodynamics," *Anesthesiology*, vol. 90, pp. 1502–1516., June 1999.

[29] C. F. Minto, T. W. Schnider, T. D. Egan, E. Youngs, H. J. M. Lemmens, P. L. Gambus, V. Billard, J. F. Hoke, K. H. P. Moore, D. J. Hermann, K. T. Muir, J. W. Mandema, and S. L. Shafer, "Influence of Age and Gender on the Pharmacokinetics and Pharmacodynamics of Remifentanil: I. Model Development," *Anesthesiology*, vol. 86, pp. 10–23, Jan. 1997.

[30] C. F. Minto, T. W. Schnider, T. G. Short, K. M. Gregg, A. Gentilini, and S. L. Shafer, "Response Surface Model for Anesthetic Drug Interactions," *Anesthesiology*, vol. 92, pp. 1603–1616, June 2000.

[31] D. J. Eleveld, P. Colin, A. R. Absalom, and M. M. R. F. Struys, "Pharmacokinetic–pharmacodynamic model for propofol for broad application in anaesthesia and sedation," *British Journal of Anaesthesia*, vol. 120, pp. 942–959, May 2018.

[32] D. J. Eleveld, J. H. Proost, H. Vereecke, A. R. Absalom, E. Olofsen, J. Vuyk, and M. M. R. F. Struys, "An Allometric Model of Remifentanil Pharmacokinetics and Pharmacodynamics," *Anesthesiology*, vol. 126, pp. 1005–1018, June 2017.

[33] T. W. Bouillon, J. Bruhn, L. Radulescu, C. Andresen, T. J. Shafer, C. Cohane, and S. L. Shafer, "Pharmacodynamic Interaction between Propofol and Remifentanil Regarding Hypnosis, Tolerance of Laryngoscopy, Bispectral Index, and Electroencephalographic Approximate Entropy," *Anesthesiology*, vol. 100, pp. 1353–1372, June 2004.

[34] A. Krieger, N. Panoskaltsis, A. Mantalaris, M. C. Georgiadis, and E. N. Pistikopoulos, "Modeling and Analysis of Individualized Pharmacokinetics and Pharmacodynamics for Volatile Anesthesia," *IEEE Transactions on Biomedical Engineering*, vol. 61, pp. 25–34, Jan. 2014.

[35] G. Besançon, *Nonlinear Observers and Applications*. No. 363 in Lecture Notes in Control and Information Sciences, Berlin Heidelberg: Springer, 2007.

[36] R. Labbe, *Kalman and Bayesian Filters in Python*. 2014.

[37] E. Petri, R. Postoyan, D. Astolfi, D. Nešić, and V. Andrieu, "Towards improving the estimation performance of a given nonlinear observer: A multi-observer approach," in *2022 IEEE 61st Conference on Decision and Control (CDC)*, pp. 583–590, Dec. 2022.

[38] M. Alamir, "Nonlinear Moving Horizon Observers: Theory and Real-Time Implementation," in *Nonlinear Observers and Applications*, pp. 139–179, Springer, 2007.

[39] J. B. Rawlings, D. Q. Mayne, and M. Diehl, *Model Predictive Control: Theory, Computation, and Design*. Nob Hill Publishing, LLC Cheryl M. Rawlings, 2009.

[40] M. Schiavo, F. Padula, N. Latronico, L. Merigo, M. Paltenghi, and A. Visioli, "Performance evaluation of an optimized PID controller for propofol and remifentanil coadministration in general anesthesia," *IFAC Journal of Systems and Control*, vol. 15, p. 100121, Mar. 2021.

[41] J. A. E. Andersson, J. Gillis, G. Horn, J. B. Rawlings, and M. Diehl, "CasADi: A software framework for nonlinear optimization and optimal control," *Mathematical Programming Computation*, vol. 11, pp. 1–36, Mar. 2019.

[42] B. Aubouin-Pairault, M. Fiacchini, and T. Dang, "PAS: A Python Anesthesia Simulator for drug control," *Journal of Open Source Software*, vol. 8, p. 5480, Aug. 2023.

[43] A. Zorrilla-Vaca, R. J. Healy, C. L. Wu, and M. C. Grant, "Relation between bispectral index measurements of anesthetic depth and postoperative mortality: A meta-analysis of observational studies," *Canadian Journal of Anaesthesia = Journal Canadien D'anesthesie*, vol. 64, pp. 597–607, June 2017.

[44] T. Akiba, S. Sano, T. Yanase, T. Ohta, and M. Koyama, "Optuna: A Next-generation Hyperparameter Optimization Framework," in *Proceedings of the 25th ACM SIGKDD International Conference on Knowledge Discovery & Data Mining*, KDD '19, (New York, NY, USA), pp. 2623–2631, Association for Computing Machinery, July 2019.

[45] C. M. Ionescu, M. Neckebroek, M. Ghita, and D. Copot, "An Open Source Patient Simulator for Design and Evaluation of Computer Based Multiple Drug Dosing Control for Anesthetic and Hemodynamic Variables," *IEEE Access*, vol. 9, pp. 8680–8694, 2021.

[46] L. Merigo, F. Padula, N. Latronico, M. Paltenghi, and A. Visioli, "Event-based control tuning of propofol and remifentanil coadministration for general anaesthesia," *IET Control Theory & Applications*, vol. 14, no. 19, pp. 2995–3008, 2020.

[47] N. Paolino, M. Schiavo, N. Latronico, M. Paltenghi, and A. Visioli, "PK/PD model based design of PID control for closed-loop anesthesia," *IFAC Journal of Systems and Control*, vol. 27, p. 100247, Mar. 2024.